The e/h ratio of the ATLAS Hadronic Tile Calorimeter

J.A. Budagov[1], Y.A. Kulchitsky[1,2], M.V. Kuzmin[1,2], V.B. Vinogradov[1]

[1] *JINR, Dubna, Russia*

[2] *IP National Academy of Sciences, Minsk, Belarus*

Abstract

We have determined the e/h ratios of the Module-0 of the ATLAS Tile iron-scintillator barrel hadron calorimeter for five values of pseudorapidity η in the range of $-0.55 \leq \eta \leq -0.15$ for the beam energy range from 10 GeV to 300 GeV on the basis of the July 1999 test beam data. These e/h ratios demonstrate independence from $|\eta|$ value. The mean value is $e/h = 1.362 \pm 0.006$. The results are compared with the existing experimental data and with some Monte Carlo calculations.

1 Introduction

This work is devoted to study of the e/π and e/h ratios of the Module-0 of the ATLAS iron-scintillator tile barrel hadron calorimeter [1] on the basis of the July 1999 test beam period. In this test beam the setup has been exposed to the electron and pion beams with energies E = 10, 20, 50, 80, 100, 150, 180, 300 GeV at $\eta = -0.15, -0.25, -0.35, -0.45, -0.55$. The results are compared with the existing experimental data of TILECAL prototype modules [2], with the 1996 [3] and 1998 [4] test beam data of the Module-0 , various iron-scintillator calorimeters and with some Monte Carlo calculations.

2 Module-0 test beam setup

The setup is shown in Fig. 1. This is the Module-0 surrounded by five 1m prototype modules which are placed on a scanning table on top and at the bottom of the Module-0 with a 10 cm gap between them.
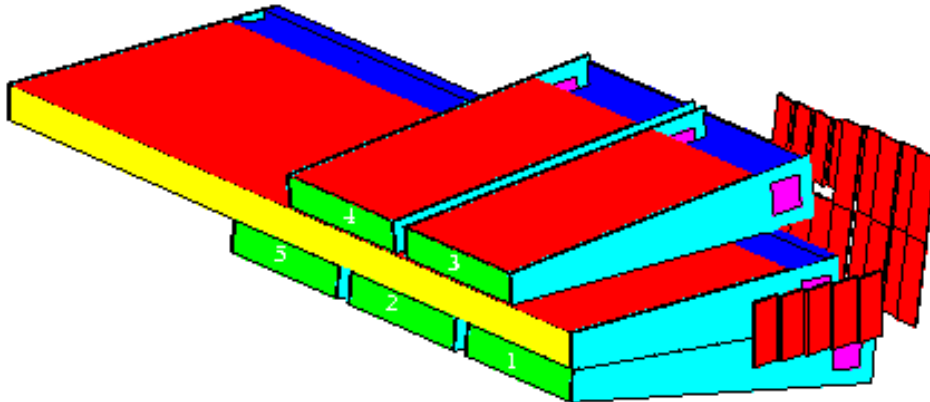

Figure 1: Sketch of the Module 0 test beam setup.

The iron structure of the Module-0 and 1m prototype modules consists of repeated "periods". Each period is 18 mm thick and consists of four layers. The first and third layers are formed by large trapezoidal steel plates (master plates), and spanning the full longitudinal dimension of the module. In the second and fourth layers, smaller trapezoidal steel plates (spacer plates) and scintillator tiles alternate . The master plates, spacer plates and scintillator tiles are 5 mm, 4 mm and 3 mm thick, respectively. The iron to scintillator ratio is 4.67:1 by volume.
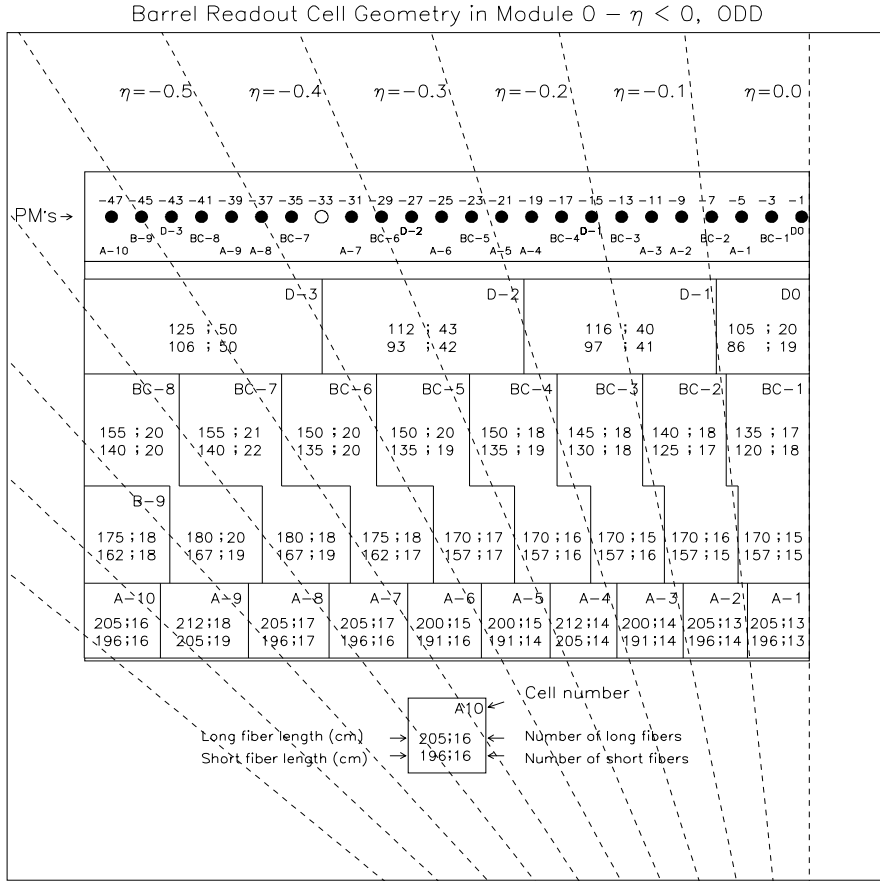
Cell−PMT configuration, fiber lengths, fiber numbs.

Figure 2: The layout of the cell geometry for Module 0.

The layout of the readout cell geometry for the Module-0 is shown in Fig. 2. The Module-0 has three depth segmentations. The thickness of the Module-0 at $\Theta = 0^o$ is 1.5 λ in the first depth sampling, 4.2 λ in the second and 1.9 λ in the third with a total depth of 7.6 λ. The Module-0 samples the shower with 11 tiles varying in depth from 97 to 187 mm. The front face area is of 560×22 cm^2.

Upstream of the calorimeter, a trigger counter telescope (S1 − S4) was installed, defining a beam spot of 2 cm in diameter. Two delay-line wire chambers (BC1 − BC2), each with Z, Y readout, allowed the impact point of beam particles on the calorimeter face to be reconstructed to better than ±1 mm . A helium Čerenkov threshold counter was used to

3

tag π-mesons and electrons for $E \leq 20 GeV$. For the measurements of
the hadronic shower longitudinal and lateral leakages back ($80 \times 80 cm^2$)
and side ($40 \times 115 cm^2$) "muon walls" were placed behind and on the side
of the calorimeter.

3   Event Selection

The following 8 cuts were used. The cuts 1 removed beam halo. The
cut 2 removed muons. The cuts 4, 5 and 6 carried out the electron-pion
separation, rejected pions in electron runs and electron in pion runs.
The cut 4 is connected with Cherenkov counter amplitude for $E_{beam} \leq$
20 GeV. Cut 5 is the relative shower energy deposition in the first two
calorimeter depths:

$$C_i = \sum_{selected\ i}\ \sum_{j=3} \sum_{k=1}^{2} \sum_{l=1}^{2} E_{ijkl}/E_{beam}\ . \tag{1}$$

The indexes i and k in E_{ijkl} determine the regions of electromagnetic
shower development. The cut 6 is related with the lateral shower spread

$$E_{cut} = \frac{\sqrt{\sum_c (E_c^{\alpha} - \sum_c E_c^{\alpha}/N_{cell})^2}}{\sum_c E_c^{\alpha}}\ , \tag{2}$$

where $1 \leq c \leq N_{cell}$, N_{cell} is the used cells number, $\alpha = 0.6$. Due to
application of these cuts two groups of events are clearly separated: with
incident electrons and with incident pions.

Special attention has been devoted to rejecting of the events with the
energy leakage. We have used for this cuts 6 – 8. The cut 6 rejected the
events in which N_{BMW} is greater than 3, where N_{BMW} is the number
of counters inside the Back Muon Wall (BMW) hodoscope with signal
greater than 0.7 mip (Fig. 3A). The cut 7 rejected the events in which
the relative energy deposition in the first depth sampling is less than
0.15 (Fig. 3B). The cut 8 rejected the events in which the total relative
energy deposition in the first and second samplings and in 1m prototype
modules is smaller than 0.4 – 0.6 depending from the beam energy.
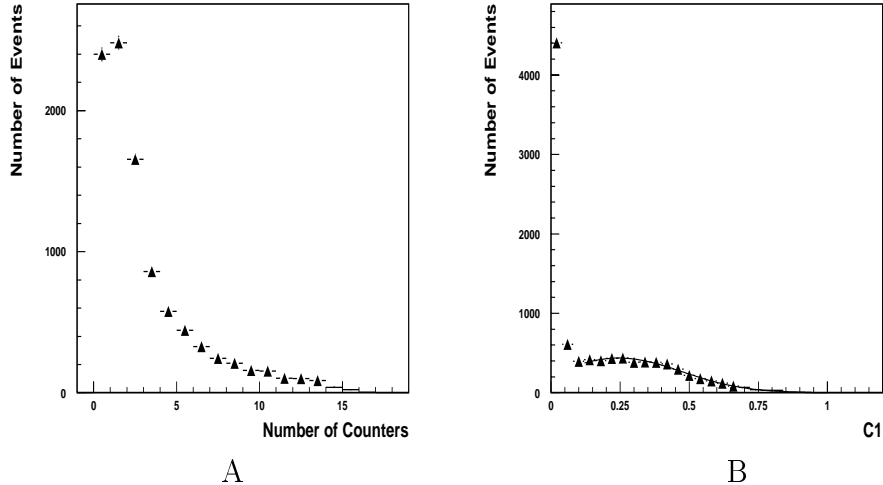
4

Figure 3: A) The N_{BMW} distribution for $E_{beam} = 300\ GeV$ at $\eta = -0.15$.
B) The $C1 = E_{s1}/E_{beam}$ distribution for $E_{beam} = 300\ GeV$ at $\eta = -0.15$.

4   Electron Response

As to the electron response our calorimeter is complicated object. It may be imagined as a continuous set of calorimeters with the variable absorber and scintillator thicknesses (from $t = 94$ to 28 mm and from $s = 20$ to 6 mm for $9^o \leq \Theta \leq 30^o$), where t and s are the thicknesses of absorber and scintillator respectively.

Therefore an electron response ($R_e = E_e/E_{beam}$) is function of E_{beam}, Θ and Z. The energy response spectrum for given run (beam has the transversal spread $\pm 20\ mm$) as a rule is non-Gaussian.

As an example, Fig. 4 shows the normalized electron response for $E_{beam} = 80\ GeV$ and $\eta = -0.15$ as a function of the impact point Z coordinate. One can see the periodical structure of the response with 18 mm period. The mean values (parameter P_2) and the amplitudes (parameter P_1) of such spectra have been extracted by fitting the sine function:

$$f(Z) = P_2 + P_1 \sin\left(2\pi Z/P_3 + P_4\right) . \tag{3}$$

Fig. 5 shows the mean normalized electron response as a function of energy at $\eta = -0.45$. Fig. 6 shows the same for the rest values of η. The spreads do not exceed 2% except several points.
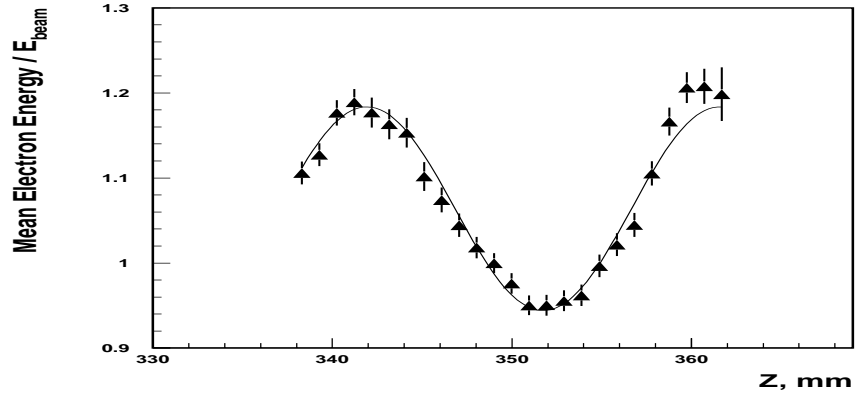
5

Figure 4: The normalized electron response (E/E_{beam}) for the beam energy of 80 GeV at $\eta = -0.15$ as a function of impact point Z coordinate.
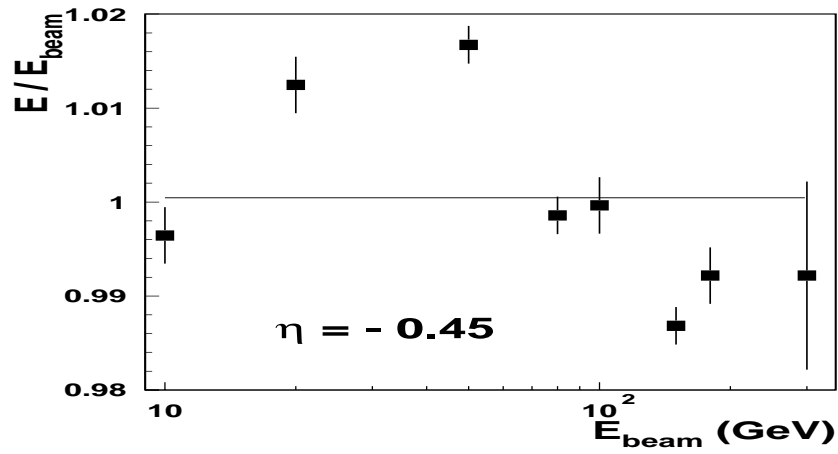

Figure 5: The mean normalized electron response (E_e/E_{beam}) as a function of the beam energy at $\eta = -0.45$. Only statistical errors are shown.
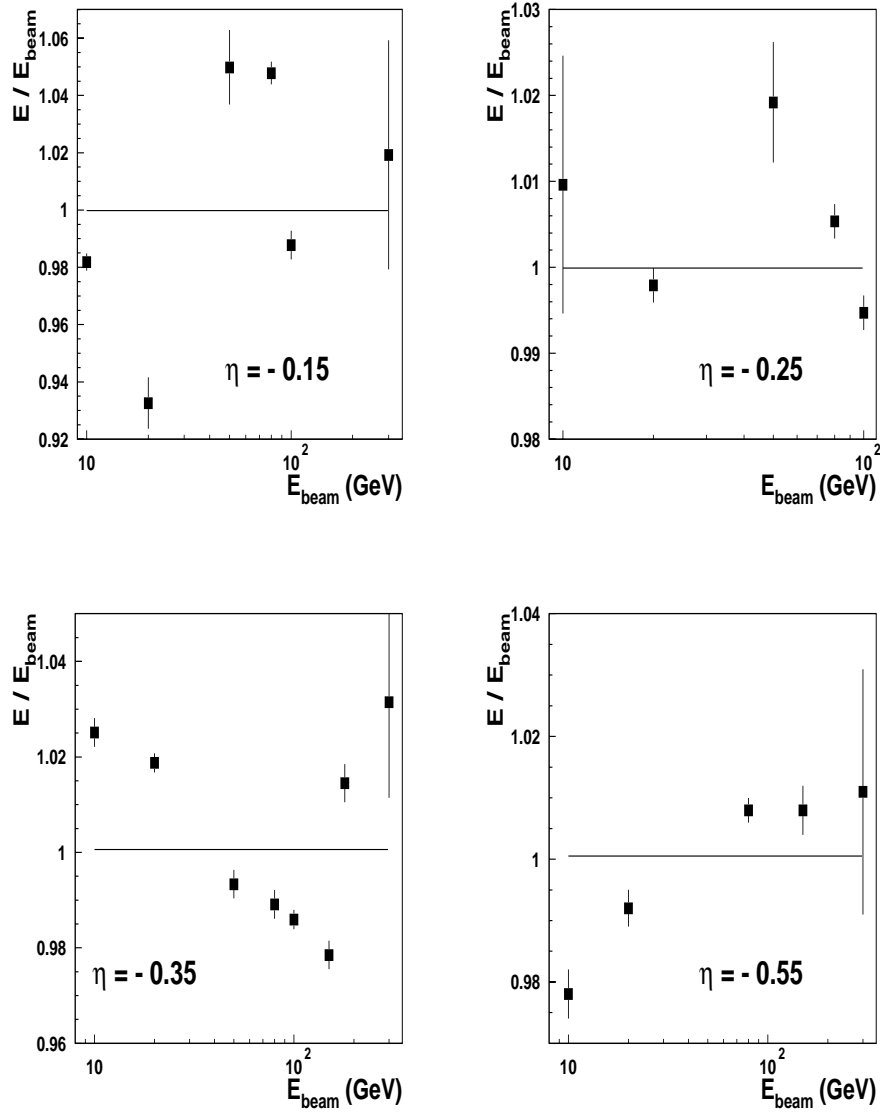
6

Figure 6: The mean normalized electron response (E_e/E_{beam}) as a function of the beam energy at $\eta = -0.15, -0.35$ (left column, up to down) and $\eta = -0.25, -0.55$ (right column, up to down). Only statistical errors are shown.

5   Pion Response

Due to wider hadronic showers contrary to the electromagnetic ones the Z dependencies for pions are flat and the energy distributions have the Gaussian behaviour with some tails.
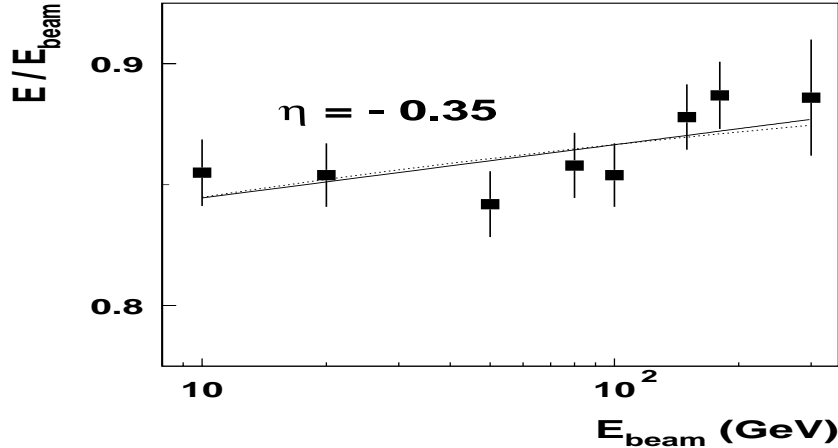

Figure 7: The mean normalized pion response (E_π/E_{beam}) as a function of the beam energy at $\eta = -0.35$. The solid (dashed) lines are the fits with the Wigmans (Groom) parameterization of $f_{\pi^o}(E)$.

Fig. 7 shows the mean normalized pion response (E_{pion}/E_{beam}) s a function of the beam energy at $\eta = -0.35$. Fig. 8 shows the same for the rest values of η. As can be expected, since the e/π ratio is not equal to 1, the mean normalized pion response increases with the beam energy increasing.

6   The e/h Ratio

The responses obtained for e and π give the possibility to determine the e/h ratio, an intrinsic non-compensation of a calorimeter. In our case the e/π ratios reveal complicated structures $e/\pi = f(E, \Theta, Z)$. Fig. 9 shows the typical e/π ratio as a function of Z coordinate. Such dependencies have been fitted by the sine function.

The extracted mean e/π ratios are shown in Fig. 10 for $\eta = -0.35$ and in Fig. 11 for the rest values of η as a function of the beam energy.
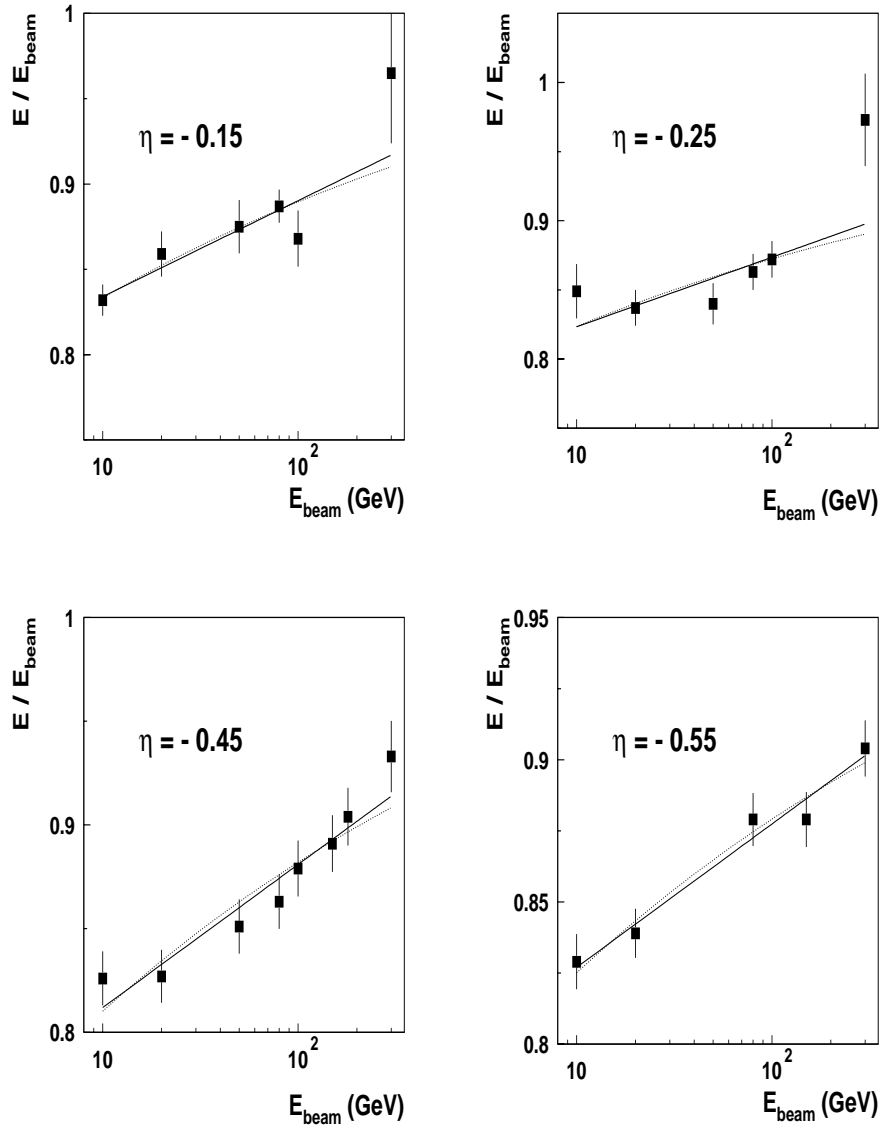
8

Figure 8: The mean normalized pion response (E_π/E_{beam}) as a function of the beam energy at $\eta = -0.15, -0.45$ (left column, up to down) and $\eta = -0.25, -0.55$ (right column, up to down). The solid (dashed) lines are the fits with the Wigmans (Groom) parameterization of $f_{\pi^o}(E)$.
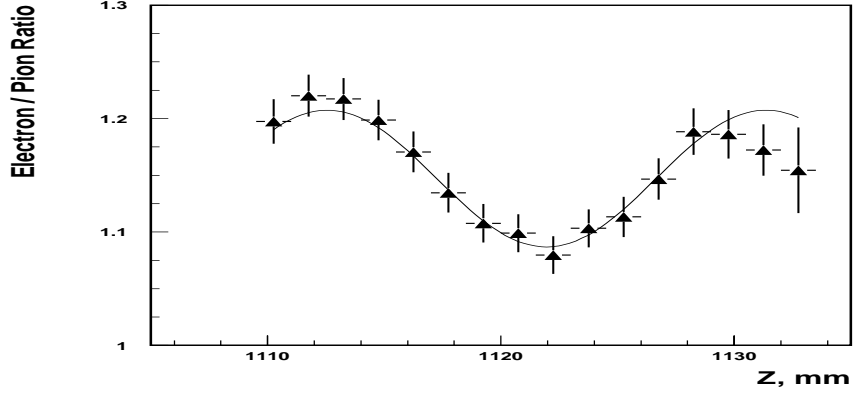
9

Figure 9: The e/π ratio as a function of Z coordinate for 100 GeV at η = - 0.45.

The errors include statistical errors and a systematic error of 1 %, added in quadrature.

For extracting the e/h ratio we have used two methods: the standard e/π method and the pion response method. In the first method, the relation between the e/h ratio and the e/π ratio is:

$$e/\pi = \frac{<E_e>}{<E_\pi>} = \frac{e/h}{1 + (e/h - 1) \cdot f_{\pi^0}} \ , \tag{4}$$

where f_{π^0} is the average fraction of the energy of the incident hadron going into π^0 production [5].

In the second method, the relation between the e/h ratio and the pion response, $<E_\pi>$, is:

$$\frac{<E_\pi>}{E_{beam}} = \frac{e}{e/h}(1 + (e/h - 1) \cdot f_{\pi^0}) \ , \tag{5}$$

where e is the efficiency for the electron detecting. Note that usually this is two parameters fit with parameters e and e/h. In principle, the e value can be determined from the ratio $e = <E_e>/E_{beam}$.

There are two analytic forms for the intrinsic π^o fraction suggested by Groom [6]

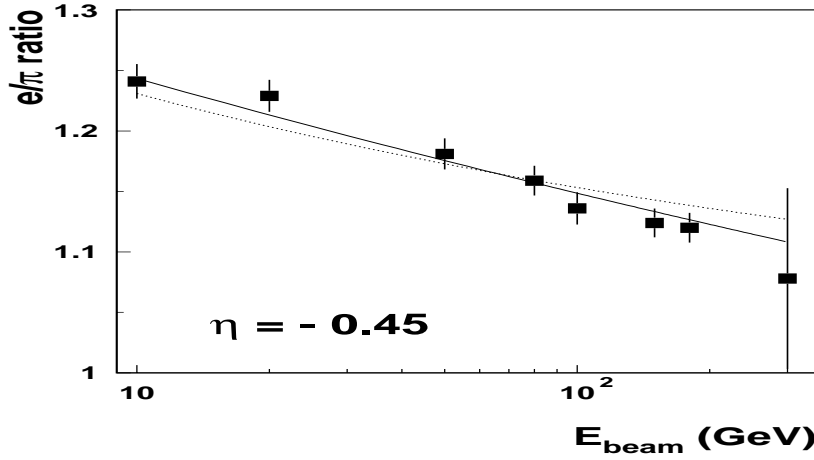$$f_{\pi^o} = 1 - \left(\frac{E}{E'_o}\right)^{m-1} \tag{6}$$

Figure 10: The e/π ratio as a function of the beam energy for $\eta = -0.45$. The solid (dashed) lines are the fits with the Wigmans (Groom) parameterization of $f_{\pi^o}(E)$.

and Wigmans [5]

$$f_{\pi^o} = k \cdot ln\left(\frac{E}{E'_o}\right) \ , \tag{7}$$

where $E'_o = 1$ GeV, $m = 0.85$, $k = 0.11$.

We used both parameterizations. The e/π ratio and the pion response and its fitting of the expressions (4), (5) with the Wigmans (solid line) and Groom (dashed line) parameterizations of $f_{\pi^o}(E)$ are shown in Fig. 7, Fig. 8, Fig. 10 and Fig. 11 as a function of the beam energy.

Fig. 12A show the e/h ratios obtained by the e/π method with the Wigmans (black boxes) and Groom (black circles) parameterizations of $f_{\pi^o}(E)$. They are compatible within errors. The e/h ratios obtained by the pion response method with the Wigmans (open boxes) and Groom (open circles) parameterizations of $f_{\pi^o}(E)$ are shown in Fig. 12B. They are compatible too. As can be seen the errors of the e/h ratios in the pion response method are about five times more than in the e/π method.

We have investigated the effect of the energy leakage on the obtained e/h ratios. Fig. 13 shows the e/h ratios corrected to the energy leakage (cuts 6 − 8) and uncorrected ones. One sees that absence of proper rejecting of events with the energy leakage leads to overestimated values of the e/h ratios and appearance of η dependence.

For the final results we have chosen the e/π method and the Wigmans
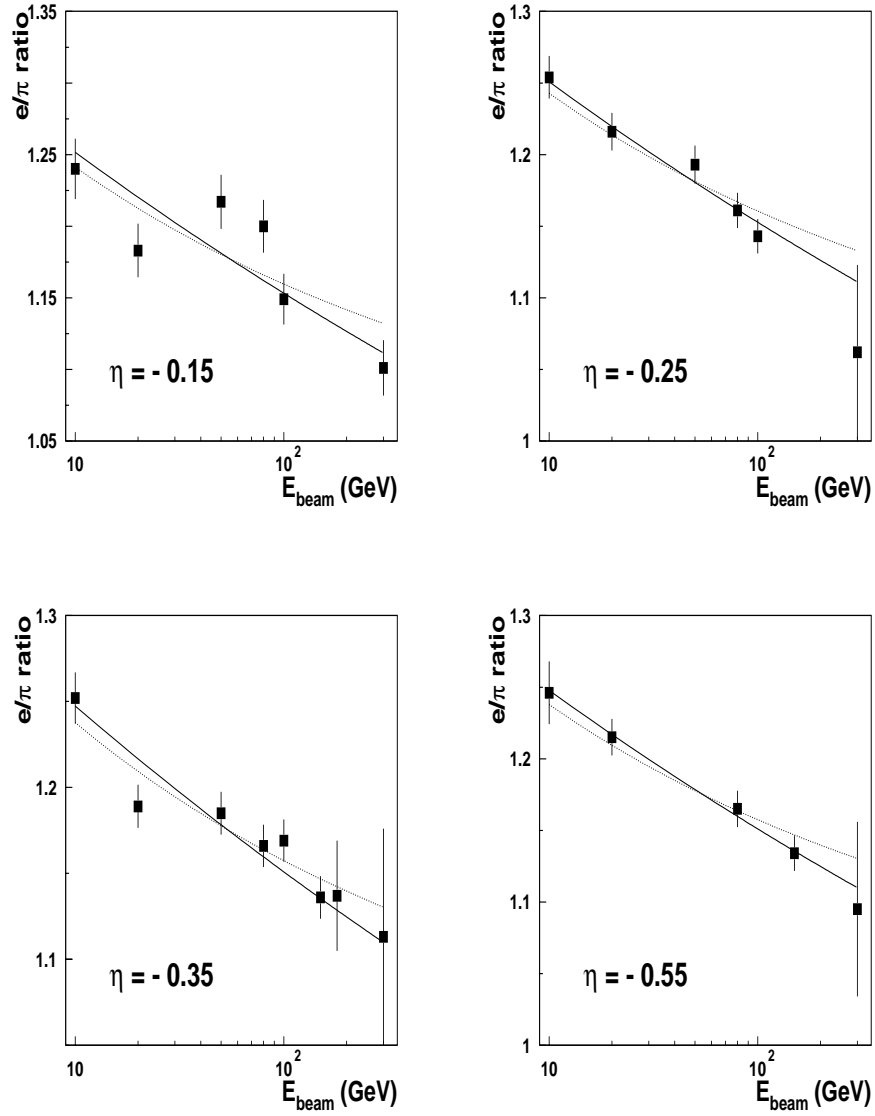
11

Figure 11: The e/π ratio as a function of the beam energy at $\eta = -0.15, -0.35$ (left column, up to down) and $\eta = -0.25, -0.55$ (right column, up to down). The solid (dashed) lines are the fits with the Wigmans (Groom) parameterization of $f_{\pi^o}(E)$.
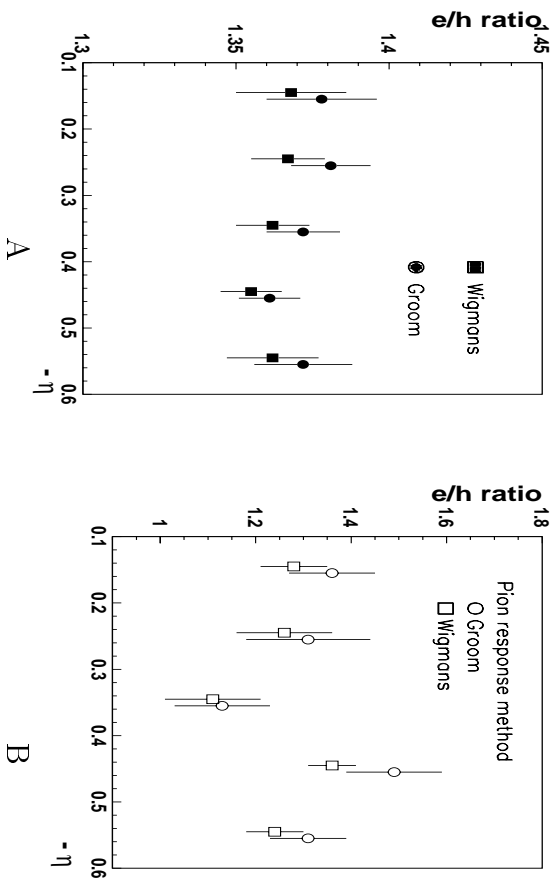
12

Figure 12: A) The e/h ratios obtained by the e/π method with the Wigmans (■) and Groom (●) parameterizations of f_{π^o}. B) The e/h ratios obtained by the pion response method with the Wigmans (□) and Groom (○) parameterizations of f_{π^o}.
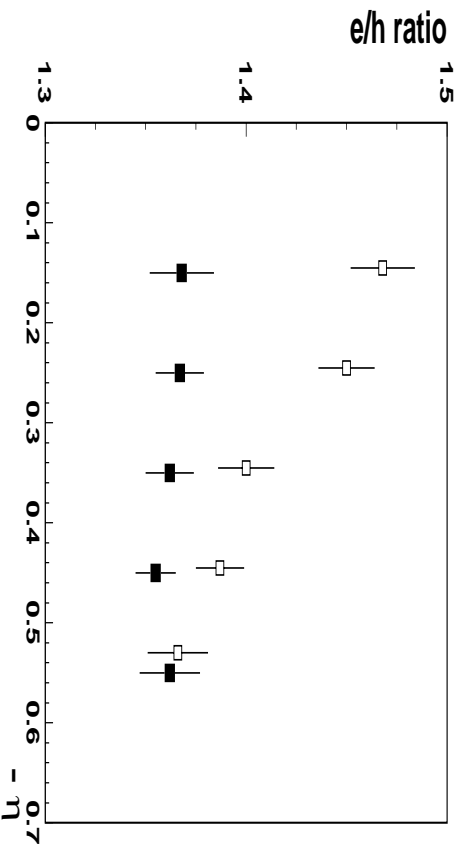

Figure 13: The e/h ratios for the Module0-99 corrected to the energy leakage (■) and uncorrected ones (□) as a function of η.

13

parameterization. The obtained values of the e/h ratios are shown in Fig. 14. These e/h ratios are in the range of about $1.35 \div 1.37$ and demon-
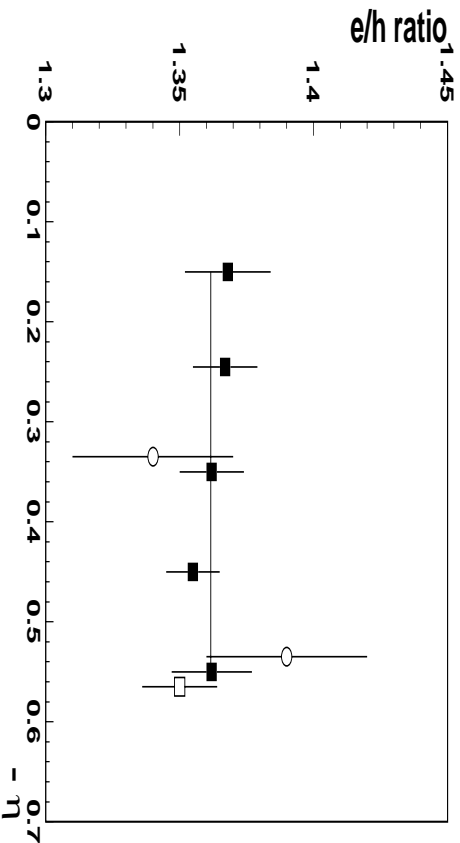

Figure 14: The e/h ratios for the Module0-99 (■), Module0-96 (□) and 1m prototype modules (○) as a function of η.

strate independence from η value. The mean value is $e/h = 1.362 \pm 0.006$. Note, that the systematic error is ± 0.007. The obtained results are compared in this Figure and in Table 1 with the other existing experimental data of TILECAL 1m prototype modules, with the 1996 and 1998 test beam data of the Module-0 , various iron-scintillator calorimeters with R_d in the range $4 \div 7$ and with some Monte Carlo calculations. The corresponding values of the thickness of the iron absorber (t), the thickness of the readout scintillator layers (s) and the ratio $R_d = t/s$ are also given in Table 1. One sees that the e/h ratios for the Module0-99 agree with the e/h ratios for the Module0-96 [3], for the Module0-98 [4], for the 1m prototype modules [2], for the conventional iron-scintillator calorimeters [8], [9], the Monte Carlo calculations [4], performed for the Module0, and disagree with the Monte Carlo calculations [11], [12]. But these Monte Carlo calculations are in obvious contradiction with each other. This Table also shows that the experimental e/h ratios decrease with R_d increasing as predicted by Wigmans [11].

Note that we have not used for comparison data [3] for the Module0-96 at $\eta = -0.25$ and data [4] for the Module0-98 at $\eta = -0.35$, which are distorted due to unaccounted essential energy leakage, and data of the 1m prototype modules at 10° [2] because at small angles due to alignment

Table 1: The e/h ratios for our and various iron-scintillator calorimeters. t is the thickness of the iron absorber, s is the thickness of the readout scintillator layers and the ratio $R_d = t/s$.

	$|\eta|$	Ref.	R_d	t, mm	s, mm	e/h
Bohmer		[7] **	2.8	20.	7.0	1.44±0.03
Module0-99	0.15÷0.55		4.7	94÷28	20÷6	1.362 ± 0.006
Module0-96	0.55	[3]	4.7	28	6	1.36 ± 0.014
Module0-98	0.45	[4]	4.7	33	7	1.39 ± 0.012
Module0-98	0.55	[4]	4.7	28	6	1.41 ± 0.012
1m prot.	0.36	[2]	4.7	41	9	1.34 ± 0.03
1m prot.	0.55	[2]	4.7	28	6	1.39 ± 0.03
Abramovicz		[8] **	5	25	5	1.32±0.03
Vincenzi		[9] **	5	25	5	1.32±0.03
Holder		[10] **	8.3	50.	6.0	1.18±0.02
Castillo	0.45	[4] *	4.7	33	7	1.40 ± 0.013
Wigmans		[11] *	5	25	5	1.21
Gabriel		[12] *	6.3	19	3	1.55

* Monte Carlo calculations
** The our estimate of 2 % error is given

of scintillator tiles in the staggered tile/iron geometry of these modules the essential electron and pion energy leakage is possible.

We think that the η dependence of the e/h ratios for the barrel and extended barrel Module0 observed in [4] is connected with the unaccounted longitudinal and transverse energy leakage.

7   Conclusions

The vast and detailed experimental information about the electron and pion responses and the e/h ratios as a function of the incident energy E and pseudorapidity η of the Module-0 of the ATLAS Tile Calorimeter on the basis of the July 1999 testbeam at energies E = 10, 20, 50, 80, 100, 150, 180, 300 GeV and $\eta = -0.15, \ -0.25, \ -0.35, \ -0.45, \ -0.55$ have been obtained.

The mean normalized electron responses as a function of Z coordinate are well described by the sine function. The spreads of the energy

linearity for electrons do not exceed ± 2 % except three points.

The e/h ratios have been determined using two methods: the e/π method and the pion response method and two analytic forms for the intrinsic π^o fraction suggested by Wigmans and Groom. It is shown that the e/π method allows to extract the e/h ratios with the accuracy of ± 1 % while the two-parametric pion response method with one of ± 5 %. The e/h ratios obtained, using the Wigmans and Groom parameterizations of $f_{\pi^o}(E)$, are compatible within errors.

For the final results we have used the e/h ratios determined by the e/π method with the Wigmans parameterization of $f_{\pi^o}(E)$. These e/h ratios demonstrate independence from η value. The mean value is $/h = 1.362 \pm 0.006$.

The obtained e/h ratios for the Module0-99 agree with the e/h ratios for the Module0-96 [3], for the Module0-98 [4], for the 1m prototype modules [2], for the conventional iron-scintillator calorimeters [8], [9] and the Monte Carlo calculations [4].

8 Acknowledgements

References

[1] ATLAS Collaboration, ATLAS TILE Calorimeter Technical Design Report, CERN/ LHCC/ 96-42, ATLAS TDR 3, CERN, Geneva, Switzerland, 1996.

[2] J.A. Budagov, Y.A. Kulchitsky, V.B. Vinogradov et al., JINR-E1-95-513, Dubna, Russia; ATL-TILECAL-95-72, CERN, Geneva, Switzerland.

[3] Y.A. Kulchitsky, V.B. Vinogradov, JINR-E1-99-12, Dubna, Russia; ATL-TILECAL-99-002, CERN, Geneva, Switzerland.

[4] V. Castillo, S. Gonzalez, ATL-TILECAL-99-020, CERN, Geneva, Switzerland.

[5] R. Wigmans, NIM A265 (1988) 273.

[6] D. Groom, Proceedings of the Workshop on Calorimetry for the Supercollides, Tuscaloosa, Alabama, USA, 1990.

[7] V. Bohmer et al., NIM 122 (1974) 313.

[8] H. Abramowicz et al., NIM 180 (1981) 429.

[9] M. De Vincenze et al., NIM A243 (1986) 348.

[10] M. Holder et al., NIM 151 (1978) 69.

[11] R. Wigmans, NIM A259 (1987) 389.

[12] T.A. Gabriel et al., NIM A295 (1994) 336.